Paper No.
09575

NACE INTERNATIONAL CORROSION 2009 CONFERENCE & EXPO

The Effect of Electrode Size on Electrochemical Noise Measurements and the Role of Chloride on Localized CO_2 Corrosion of Mild Steel

Xiu Jiang, Srdjan Nešić*,
Institute for Corrosion and Multiphase Technology, Department of Chemical and Biomolecular Engineering, Ohio University, Athens, OH 45701, USA

François Huet
Université Pierre et Marie Curie-Paris6, Laboratoire Interfaces et Systèmes Electrochimiques; CNRS, UPR15-LISE, 4 place Jussieu, 75252 Paris Cedex 05, France

ABSTRACT

The simultaneous fluctuations of potential noise and current noise between two nominally identical X-65 mild steel electrodes were recorded in deaerated aqueous sodium chloride solutions with concentration ranging between 1 and 20 wt % at 80°C. Electrochemical noise (EN) was obtained from both 11.6 cm^2 and 1 cm^2 coupons in 1 wt % NaCl solution to learn how the surface area affects EN measurements. Only small surface area coupons (1 cm^2) were used in 10 wt % and 20 wt % NaCl solution experiments to understand the role of Cl^- on localized corrosion processes. Linear polarization resistance measurements were conducted in each experiment to investigate the general corrosion behavior. The surface morphology of coupons was observed with a scanning electrochemical microscope (SEM). The results showed that the electrode area influenced the EN signal. Transients related to metastable pitting were best observed with 1 cm^2 coupons in 1, 10, and 20 wt % NaCl solutions, but such transients were not clearly obtained for 11.6 cm^2 coupons in the 1 wt % NaCl solution. Both statistical analysis of recorded current and potential noise and SEM analysis showed that increasing the NaCl solution concentration did not change the localized corrosion rate.

Keywords: Localized CO_2 corrosion, mild steel, electrochemical noise, electrode size, NaCl concentration

INTRODUCTION

CO_2 corrosion has been one of the most common corrosion problems in the oil and gas industry where mild steel is the mostly common used construction material for pipelines. When CO_2 dissolves into water, carbonic acid will form, which is more corrosive to mild steel than HCl at the same pH.

* E-mail address: nesic@ohio.edu (S. Nesic).

During the CO_2 corrosion processes, a corrosion product scale, mostly iron carbonate ($FeCO_3$), precipitates on the surface of the steel which could significantly reduces corrosion rate. Any damage to the corrosion product film, for example, by mechanical dissolving, chemical dissolving or the combination of both, is typically followed by a severe corrosion attack[1]. Chemical dissolving of corrosion product film by adjusting supersaturation of $FeCO_3$ to less than 1 caused localized corrosion in previous work[2].

Most work about CO_2 corrosion has been done at low salt concentrations typically in 1 - 3 wt % NaCl solutions because localized corrosion is accelerated by chloride ions at low salt concentration[3-4]. However, high salt concentrations are present in water recovered from oil and gas wells. Considerably less work[5] has been carried out at high salt concentrations despite the fact that Cl^- is widely thought to be an aggressive pitting agent in aqueous solution[6], so that the role of Cl^- on localized corrosion in CO_2 environment is unclear.

The random fluctuations of the current (potential) observed under potentiostatic (galvanostatic) control, often called electrochemical noise (EN), have received considerable attention, especially in the corrosion engineering field, since the early works of Iverson[7] and Tyagai[8]. Some advantages of EN measurements over more conventional corrosion monitoring methods are apparent. It needs no external polarization, which could influence the electrochemical reactions unlike almost all the other electrochemical techniques do. Analysis of the spontaneous fluctuations of potential and current is used for discriminating between different corrosion processes because each type of corrosion (for example general corrosion, pitting, crevice, and stress corrosion cracking) can have a characteristic “fingerprint” or “signature” in the noise signal. This “fingerprint” can be used to identify the type of corrosion that is occurring and to evaluate its severity while the traditional electrochemical techniques, such as linear polarization resistance (LPR), electrochemical impedance, etc., which average the signals in time, cannot provide such information[9-10]. Therefore, most of the work about EN has been focused on localized corrosion.

There are many factors that influence the quality of results obtained from EN, and the size of the corroding surface specimen is one of them. The exact effect of surface area on the EN will depend on the process that is generating it. For general corrosion, corrosion processes involve a large number of corrosion events of low amplitude on the whole electrode area, the power spectral density (PSD) of current noise is proportional to the surface area, while the PSD of the potential noise is inversely proportional to the surface area. Thus, large electrodes are preferable for measuring electrochemical current noise and small electrodes are preferable for measuring electrode potential noise[9-10]. However, it is unclear if this conclusion can be used for localized corrosion, for example, pitting corrosion. In addition, the choice of the electrode size is a particular challenge with respect to the use of EN for corrosion monitoring in service. When monitoring corrosion of large structures with small probes, the occurrence of localized corrosion is much less probable on the probe than on the structure. Thus it is probable that localized corrosion will occur on the structure when they are not observed on the probe[9-10]. How do the surface areas affect the EN signal if localized corrosion occurs?

In this paper, the EN was measured for different surface areas in 1% NaCl solutions to investigate the effect of surface area on the EN signal. Then the role of Cl^- on the localized corrosion processes in 1%, 10%, and 20% NaCl solutions was studied by statistical analysis of the potential and current noises and scanning electrochemical microscopy (SEM) analysis.

EXPERIMENTAL PROCEDURES

The glass cell set-up is shown in Figure 1. The glass cell was filled up with 2L of electrolyte, which consisted of distilled water with 1%, 10% and 20% NaCl (wt %), respectively. The temperature was always maintained at 80^{o}C in these experiments. Prior to each experiment, the solution was deaerated by bubbling CO_2 gas for 1 h, and this was continued throughout the experiment. The total pressure in the glass cell was 1bar. The pH was monitored with an electrode immersed in the electrolyte. Fe^{2+} concentration was measured twice a day *via* a spectrophotometric method.
Each experiment involved the following three separate experimental steps:

Step 1: Formation of a corrosion product layer
At the start of the experiment, deoxygenated aqueous sodium hydrogen carbonate was added to adjust the pH to 6.3 for the 1% NaCl solution experiment and 6.6 for the 10% and 20% NaCl solutions. A supersaturation (SS) of 150, with respect to iron carbonate, was set by injecting a deoxygenated ferrous chloride solution for each experiment. The steel coupons were inserted and the conditions were maintained for approximately 3.5 days, during which the supersaturation of the solution decreased as the precipitation and deposition of iron carbonate ($FeCO_3$) proceeded. This led to a significant reduction of the corrosion rate of the steel coupons.

Step 2. Partial dissolution of the corrosion product layer
Once the protective corrosion product layer was established, the solution pH was adjusted to 5.0 with hydrochloric acid and the saturation with respect to $FeCO_3$ was adjusted to SS = 0.04. This gave rise to dissolution of the $FeCO_3$ corrosion product. This condition was maintained for only 4 hours in order to achieve a partial dissolution of the corrosion product layer.

Step 3: Localized corrosion
Following the partial dissolution of the protective corrosion product layer, the saturation of $FeCO_3$ was then adjusted to the so-called "grey zone" [3] (0.5 ~ 2.0) using Na based ion exchange resin, where the corrosion product layer is neither bound to dissolve or precipitate. This process was kept for 6.5 days in the 1% NaCl solution experiment and 6 days in the 10% and 20% NaCl solutions.

For the 1% NaCl solution experiment, five rectangular coupons (5.08×2.29×1.02 cm) and two squared (1×1×1.02 cm) coupons of X65 mild steel specimens were inserted into the same glass cell. Two rectangular coupons (11.6 cm^2) and two 1 cm^2 coupons were used for EN measurement while three other rectangular coupons were used for SEM observation. The test duration was 10 days for this experiment. For the 10% and 20% NaCl solution experiments, only two identical squared coupons (1 cm^2 exposed to solution) were used. The test duration for these two experiments was 8 days. Prior to immersion, the specimens were polished with 240, 400 and 600 grit SiC paper, and then rinsed with alcohol.

The electrochemical measurements were performed using a Gamry Instruments PC4-series G-300 potentiostat. The zero-resistance ammeter (ZRA) mode was used for the EN measurement. Potential noise and current noise were collected simultaneously using two identical working electrodes and a reference electrode (saturated calomel electrode (SCE) for the 1% NaCl solution experiment and Ag/AgCl for the 10% and 20% NaCl solution experiments). The reference electrode was connected externally to the cell via a luggin capillary tube and a porous tip. The readings were taken with 1 s sampling intervals. A period of 1024 s was set for each noise recording run. The corresponding PSD was calculated with the periodogram method based on the fast Fourier transform[11].

A standard three-electrode setup was used for the estimation of the general corrosion rate. The linear polarization resistance (LPR) measurements were conducted by polarizing the working electrode ±5 mV vs the open-circuit potential at a rate of 0.125 mV/s. Solution resistance was measured using the EIS technique, and the measured R_p then was corrected. EIS measurement was carried out by applying an oscillating potential of ±5 mV around the free corrosion potential, to the working electrode using the frequency range 1 Hz to 10 kHz. After the specimens were removed from the cell, they were immediately rinsed, dried, and then stored in a desiccator. The surface morphology of the coupons was characterized by SEM. Pits depth was measured by Infinite Focus Microscopy for 3D optical analysis (IFM).

RESULTS AND DISCUSSION

Effect of electrode surface area on EN in 1% NaCl solution

LPR results and surface analysis.

Supersaturation of $FeCO_3$ with time in 1% NaCl solution is shown in Figure 2. Supersaturation decreased with time during the first 3.5 days (film building process) because of the gradual deposition of $FeCO_3$ scale onto the metal surface. The supersaturation was then adjusted to 0.04 for only 4 hour. The corrosion product film was partially dissolved during this process because of undersaturation of $FeCO_3$, which may initiate localized corrosion. Finally the supersaturation was adjusted to a value close to 1 (0.5 ~ 2) so no dense film formed and the existing corrosion film was not seriously dissolved.

The evolution of the corrosion rate with time in the 1% NaCl solution is shown in Figure 3. Corrosion rates were calculated from LPR measurements assuming a B constant of 0.013V/decade. It decreased during the first 3.5 days because of the film building, and then increased when the corrosion product film was partially dissolved.

The surface morphology of the metal in the presence and in the absence of the film, which was removed by using a Clarke solution, is shown in Figure 4 after 10 days of exposure in solution. Pitting was observed in both cases. The 3-D image of a typical pit on the metal after film removal is shown in Figure 5; which depth is around 41 μm.

EN results on small coupons (1 cm^2)

Typical time records of potential and current noises for 1 cm^2 coupons in the 1% NaCl solution are shown in Figure 6 and Figure 7, respectively. The typical signature of the transients related to metastable pitting for carbon steel[12] can be observed in both figures after 6 days in solution. Every rise in current noise was accompanied by a drop in potential noise, indicating the breakdown of the corrosion product layer, followed by a recovery [10]. The evolution of the current PSDs with time is shown in Figure 8. The amplitude of each PSD was multiplied by a certain factor (shown in the Figure) for more clarity. The PSD amplitude increased with time because localized corrosion is associated with larger electrochemical events than uniform corrosion[10] After 10 days it was about two decades higher than that after 3.5 days because of the occurrence of pitting corrosion, as shown in Figure 4.

In order to show the validity of the EN measurement, time records were acquired at 1 Hz and 10 Hz sampling frequencies after 3.5 days of exposure in solution. To calculate the PSD, a single time record sampled at 1 Hz was used and 10 time records sampled at 10 Hz were used. The good overlap of the PSDs at 1 Hz and 10 Hz in Figure 8 validated the EN measurement. All EN measurements reported in this paper were done according to the same procedure to ensure the validity of both the time records and PSDs.

EN results on big coupons (11.6cm^2)

Typical time records of the potential and current noises for 11.6 cm^2 coupons in the 1% NaCl solution are shown in Figure 9 and Figure 10, respectively. The signature of the transients related to metastable pitting for carbon steel cannot be clearly observed. The evolution with time of the current PSDs, each of them calculated from a single time record, is shown in Figure 11. The current PSDs were multiplied by a certain factor for more clarity. As for the small coupons, the amplitude of the current PSDs increased with time because of the progressive appearance of pitting corrosion. The shape of the current PSDs, with a low-frequency plateau and a $1/f^2$ decrease, is identical to those measured on the small coupons, indicating that pitting corrosion actually occurred after 6 days in solution. The fact that no pitting elementary transients are visible in the time records is due to the large number of pitting events that give overlapping elementary current transients.

Comparison of EN results on small and large coupons.

The evolution with time of the standard deviation (SD) of the current noise, calculated after removal of the DC drift in the time domain for the 11.6 cm^2 and 1 cm^2 coupons in the 1% NaCl solution is shown in Figure 12. A higher SD is obtained for the large coupons during the whole experiment duration.

For general corrosion, the SD of the current noise is proportional to the square root of the surface area[12]. However, it is unclear whether this conclusion can be used for localized corrosion, such as pitting corrosion, or not. The ratio σ_1/σ_2, where σ_1 and σ_2 denote the SD of the current noise of the large and small coupons, respectively, is compared to the square rooted ratio of the surface areas $\sqrt{11.6/1} = 3.4$ in Figure 13. All the ratio values, except for the film partially dissolving process (4th hour), are close to 3.4, which indicates that the SD of the current noise was proportional to the square root of the surface area for general corrosion and pitting corrosion. The reason why the ratio is not around 3.4 during the partial dissolution process needs further investigation.

The fact that the typical transients related to metastable pitting for carbon steel were observed on the 1 cm^2 coupons (Figures 6 and 7) while no such transients were clearly observed on the 11.6 cm^2 coupons (Figures 9 and 10) can be explained with the help of Figure 14 [9]. It shows simulated time records of exponentially transients occurring randomly (Poisson process) at an average rate of $\lambda_1 = 1$ s^{-1} and $\lambda_2 = 100$ s^{-1}, and their corresponding PSDs. It is clear that increasing the transient rate leads to a random signal in which the shape of the exponential transient is no longer visible. It is therefore impossible to detect the exact shape of the transients for the large coupons. However, for such a Poisson process, increasing the transient rate does not change the shape of the PSD, only its amplitude increases by a factor λ_2/λ_1.

Thus, the smaller surface area electrode produces transients and allows a clearer identification of the current transients related to localized corrosion events.

EN results in 10% and 20% NaCl solutions

Typical transients related to metastable pitting corrosion were not clearly observed in the EN time records for the11.6 cm^2 coupons in both 10% and 20% NaCl solutions,[2] as in the 1% NaCl solution (Figures 9 and 10). Two additional experiments were carried out on small surface coupons (1 cm^2) in the

10% and 20% NaCl solutions to assess our above conclusion that the transients can be best observed on small coupons.

Typical time records and surface morphology of the steel surface before and after removal of the corrosion product film using the Clarke solution are shown in Figure 15 and Figure 16 for the 10% NaCl solution, and in Figure 17 and Figure 18 for the 20% NaCl solution. Film failure areas on the metal surface can be observed in Figure 15(a) and Figure 17(a). After film removal, pits could be observed, as shown in Figure 15(b) and Figure 17(b).

Current noise is usually considered to be produced by a large number of current "sources" or corrosion "events" on the steel surface. Typical current transients related to metastable pitting corrosion for mild steel were observed after 4 days in the 10% NaCl solution (Figure 16) and after 6.1 days in the 20% NaCl solution (Figure 18). This further proved that, as in the 1% NaCl solution, the electrode surface area had a big influence on the EN signal: current transients can only be detected in the time domain on coupons of small surface area.

The role of Cl^- ions in localized CO_2 corrosion

Pitting corrosion in the 1%, 10%, and 20% NaCl solutions was observed in Figure 4, Figure 15 and Figure 17 showing the surface morphology of the coupons. Typical transients related to metastable pitting corrosion of mild steel were detected in the EN time records for the small surface coupons (1 cm^2) for each NaCl solution concentration in Figure 7, Figure 16 and Figure 18. Therefore, pitting corrosion occurred for the whole range of NaCl concentrations. In order to understand the role of the chloride ions in the localized corrosion process, the EN and surface morphology were further analyzed.

The maximum localized corrosion penetration rate could be calculated from the maximum pit depth measured by Infinite Focus Microscopy for 3D optical analysis (IFM). A comparison of the general corrosion rate and maximum localized corrosion rate averaged over an 8 day exposure for different NaCl solutions is presented in Figure 19. In all cases, the final general corrosion rate is around 0.5 mm/y and the maximum time-averaged localized corrosion rate is around 2 mm/y. Neither of them changed with increasing NaCl concentrations. One can therefore conclude that NaCl affects neither the general corrosion rate magnitude and trend nor the morphology and magnitude of the localized attack.

CONCLUSIONS

1. Localized corrosion was observed at each NaCl solution concentration.
2. The chloride concentration had no significant effect on the general CO_2 corrosion rate and on the localized corrosion rate, under the conditions studied.
3. The EN technique was successful in providing *in-situ* information about the evolution of the localized CO_2 corrosion process. Current and potential transients related to metastable pitting can be best observed on small coupons (≈ 1 cm^2).

ACKNOWLEDGMENTS

The authors would like to acknowledge the companies who provided the financial support and technical guidance for this project. They are BP, Champion Technologies, Clariant, ConocoPhillips, Tenaris, Chevron, BAKER HUGHES, Baker Petrolite, PTTEP, Eni, OXY, ExxonMobil, Mi SWACO, NALCO, Saudi Aramco, Shell, Columbia Gas Transmission, and Total.

REFERENCES

1.V.Ruzic, "Mechanisms of protective $FeCO_3$ film remove in single-phase flow-accelerated CO_2 corrosion of mild steel", dissertation, The University of Queensland, 2005.

2. X.Jiang, S.Nesic, "Electrochemical Investigation of the Role of Cl^- on Localized CO_2 Corrosion of Mild Steel", 17th International Corrosion Congress, 2008

3.Y.F.Sun, K.Gorge, S.Nesic, "The effect of Cl^- and acetic acid on localized CO_2 corrosion in wet gas flow" Corrosion/2003, Paper 03327. (Houston, TX: NACE, 2003)

4. X.Jiang, Y.G.Zheng, D.R.Qu, W.Ke, Corrosion Science 48(2006) 3091

5. H.T.Fang, "Low temperature and high salt concentration effects on general CO_2 corrosion for carbon steel", Thesis, Ohio university, 2006.

6. M.Ergun and A.Y.Turan, Corrosion Science, 32(10) (1991) 1137

7. W.P. Iverson, Journal of Electrochemical Society, 115(1968):617

8. V.A.Tyagai, Electrochimica Acta, 16(1971):1647.

9. F. Huet, "The electrochemical noise technique", in "Analytical Methods in Corrosion Science and Engineering", eds. P. Marcus and F.Mansfeld, Taylor & Francis, CRC Press, Series: Corrosion Technology, Volume 22, p. 507-570 (2006).

10. R.Cottis, S.Turgoose, "Electrochemical Impedance and Noise", NACE international, Chapter 7, 1999.

11.U.Bertocci, J.Frydman, C.Gabrielli, F.Huet, M.Keddam, Analysis of electrochemical noise by power spectral density applied to corrosion studies - Maximum entropy method or fast Fourier transform?, J. Electrochem. Soc., 145(8) (1998), 2780-2786 .

12. R.Cottis, "Interpretation of electrochemical noise data", Corrosion 57(3) (2000)265

Table 1 Chemical composition of X-65 mild steel

	C	Mn	Si	P	S	Cr	Cu	Ni	Mo	Al
X-65	0.065	1.54	0.25	0.013	0.001	0.05	0.04	0.04	0.007	0.041

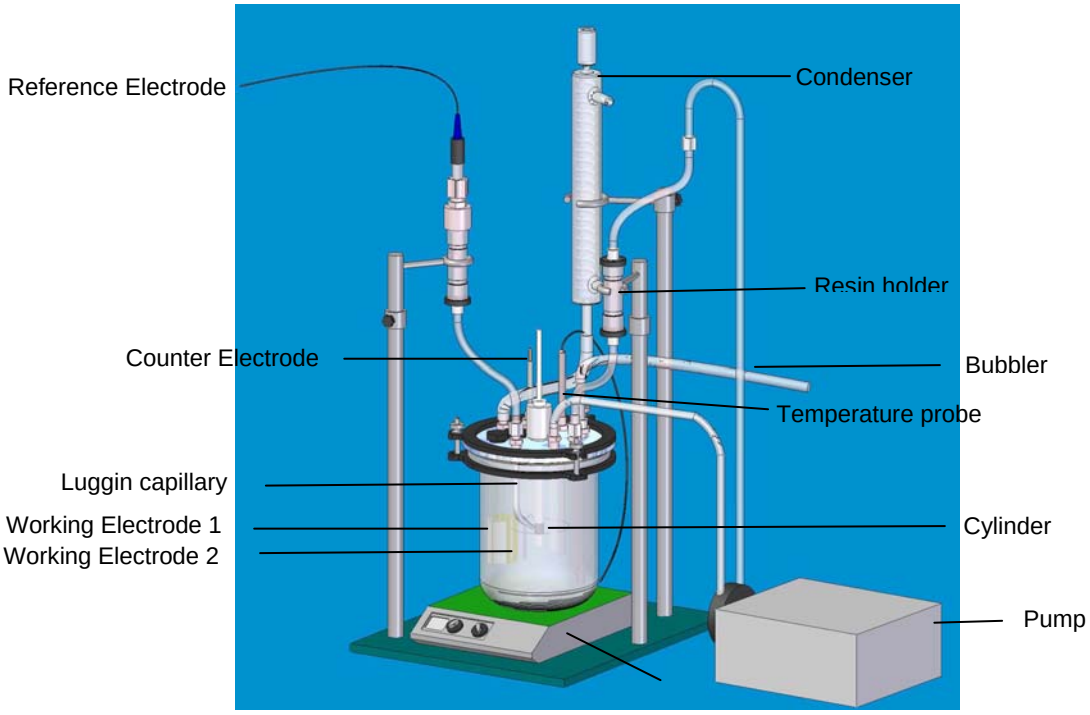

Figure 1. Glass cell set-up

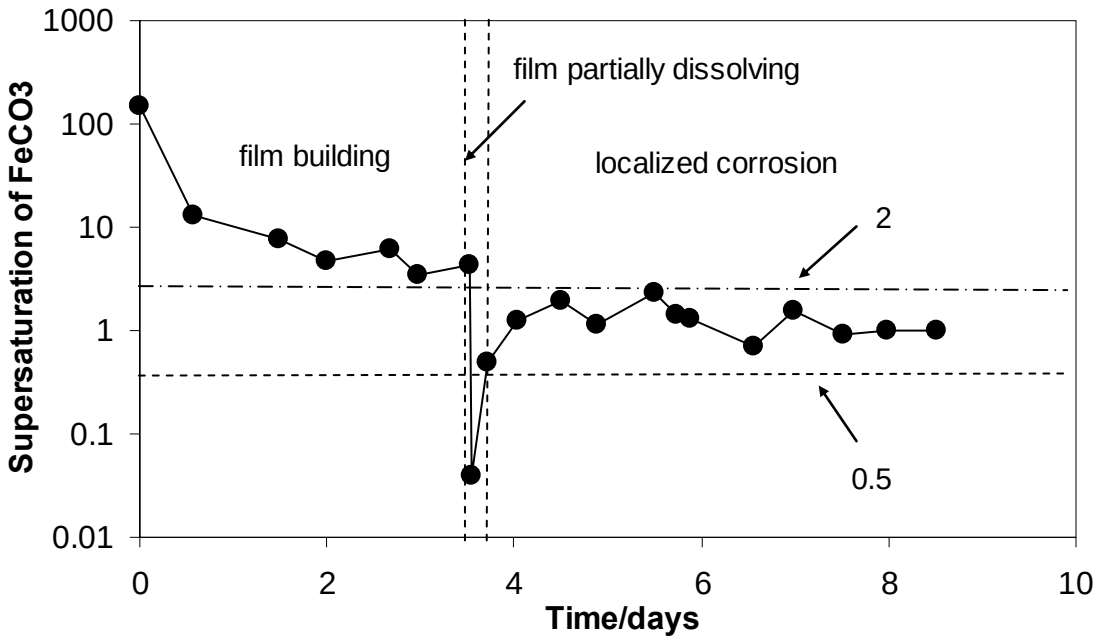

Figure 2. Supersaturation of $FeCO_3$ with time in 1% NaCl solution

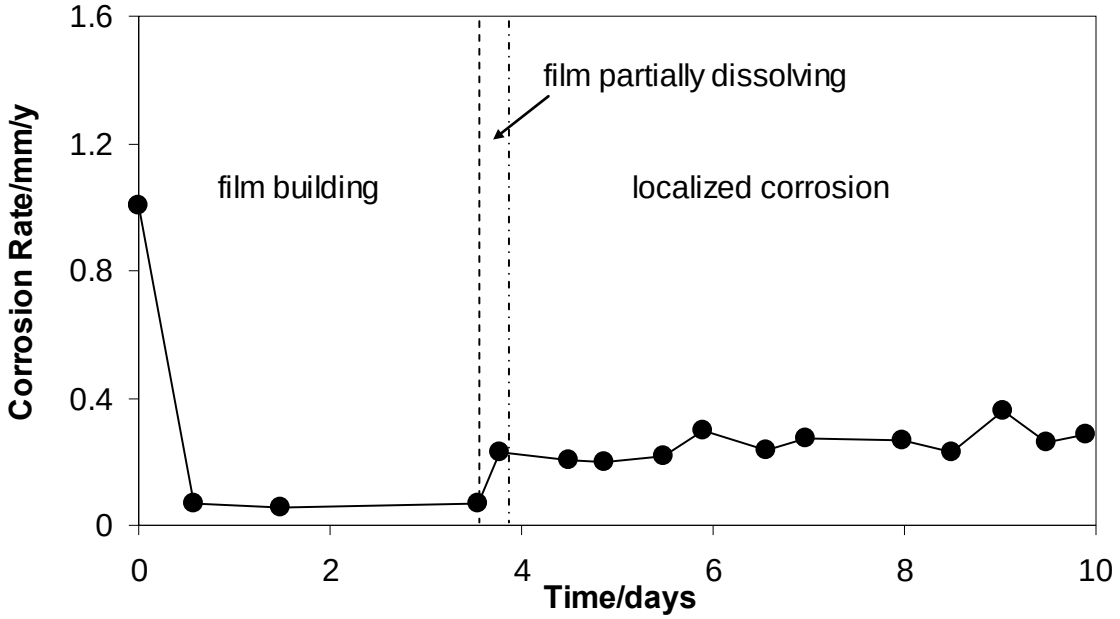

Figure 3. Corrosion rate with time in 1% NaCl solution, measured using LPR

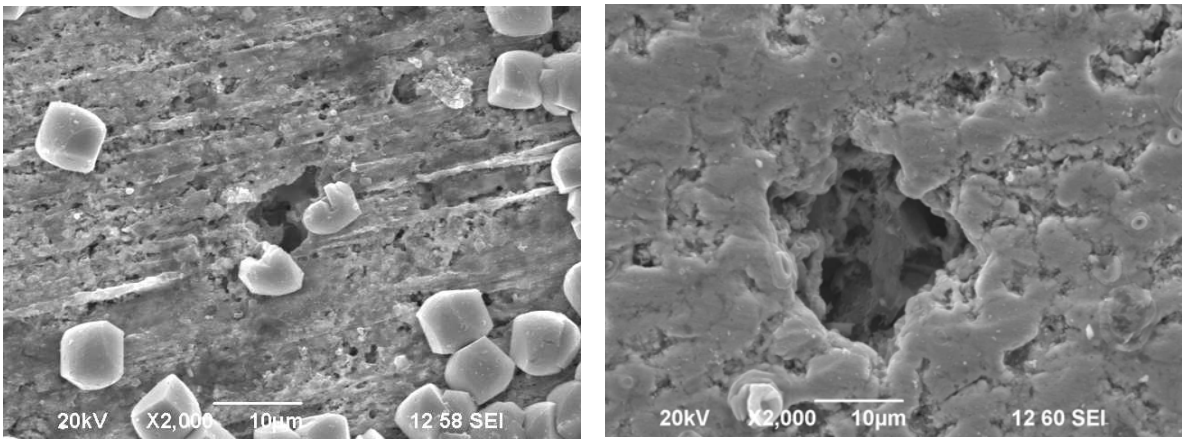

(a) (b)

Figure 4. Surface morphology for metal with film ((a)) and after film removal by using Clarke solution ((b)) after 10 days in 1% NaCl solution

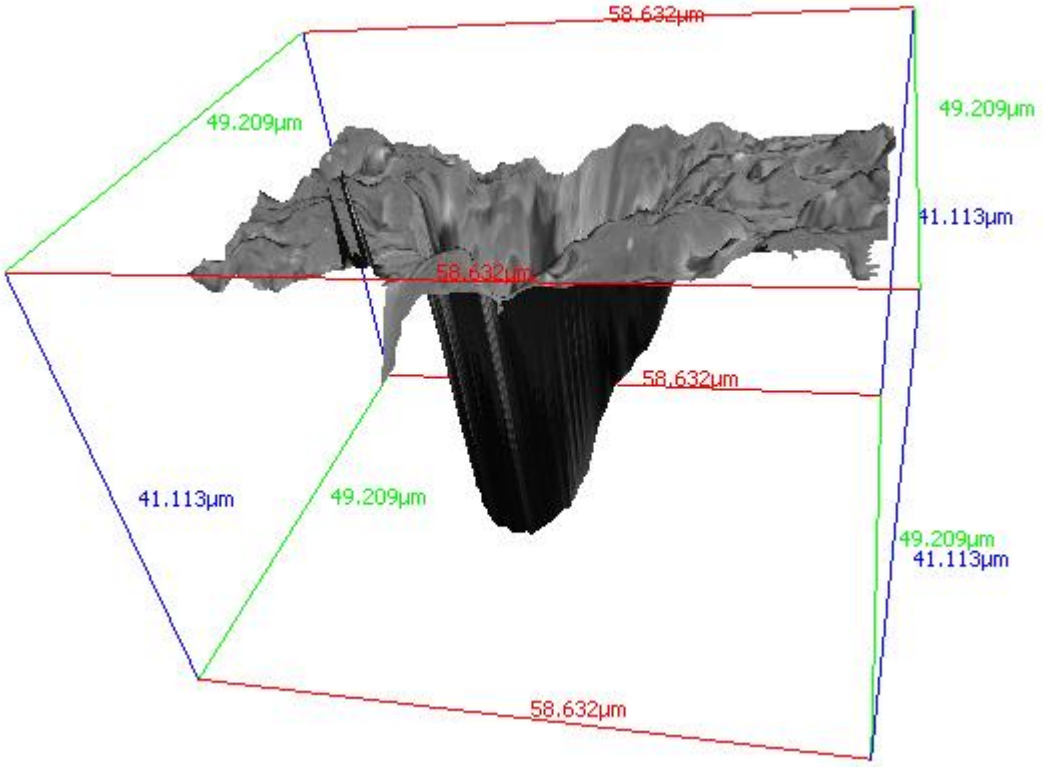

Figure 5. 3-D image of a pit found after film removal by using Clarke solution after 10 days

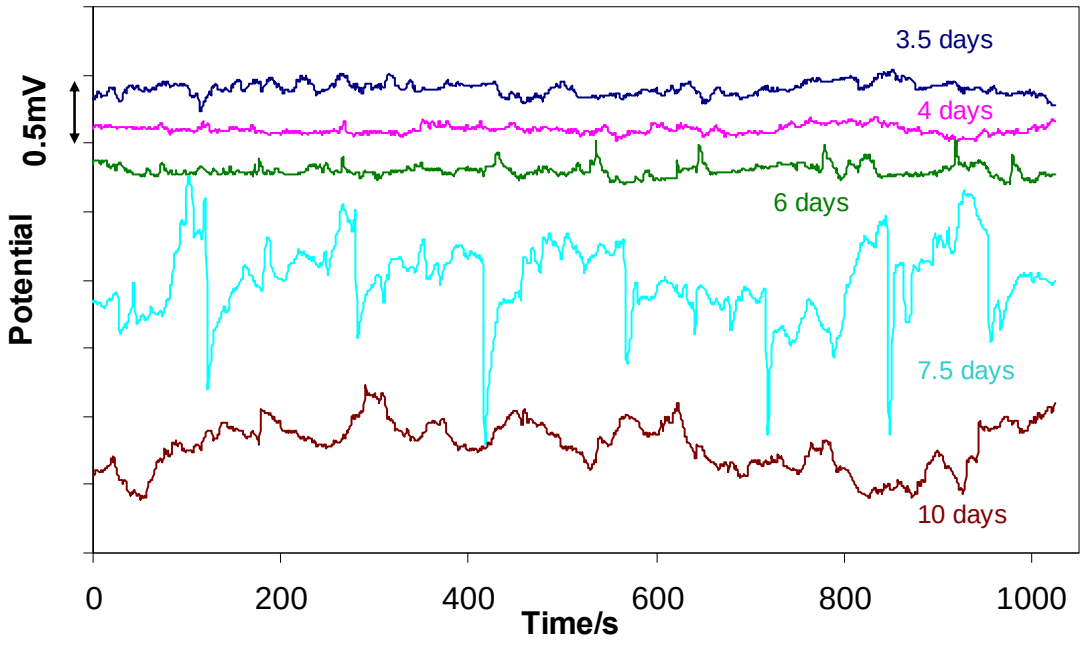

Figure 6. Potential noise with time for 1cm^2 coupons in 1% NaCl solution after removing the DC drift using the polynomial fitting method

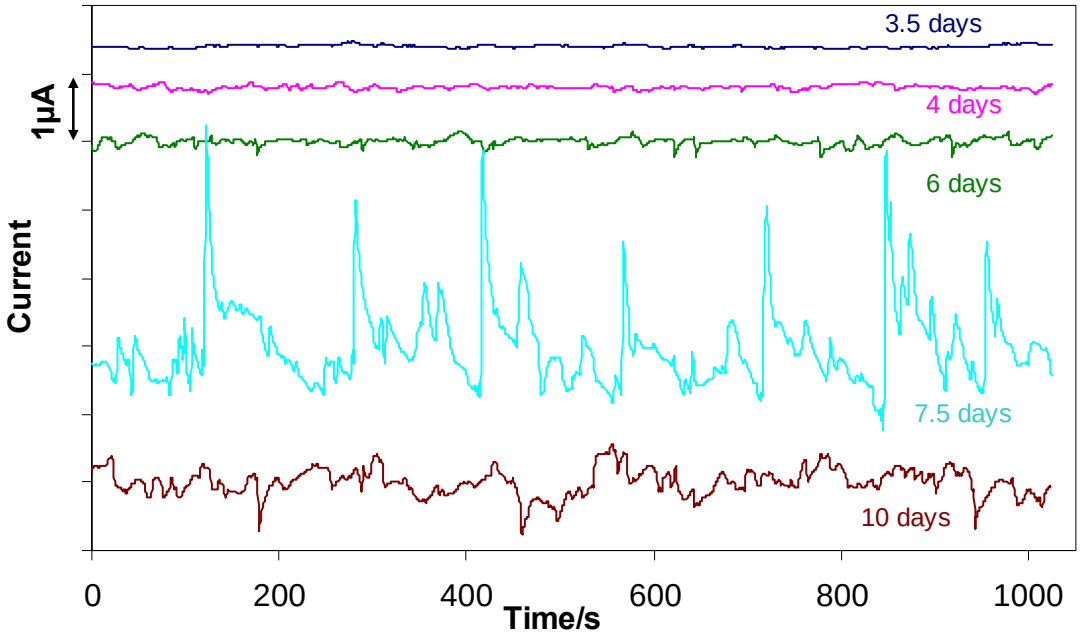

Figure 7. Current noise with time for 1cm^2 coupons in 1% NaCl solution after removing the DC drift using the polynomial fitting method

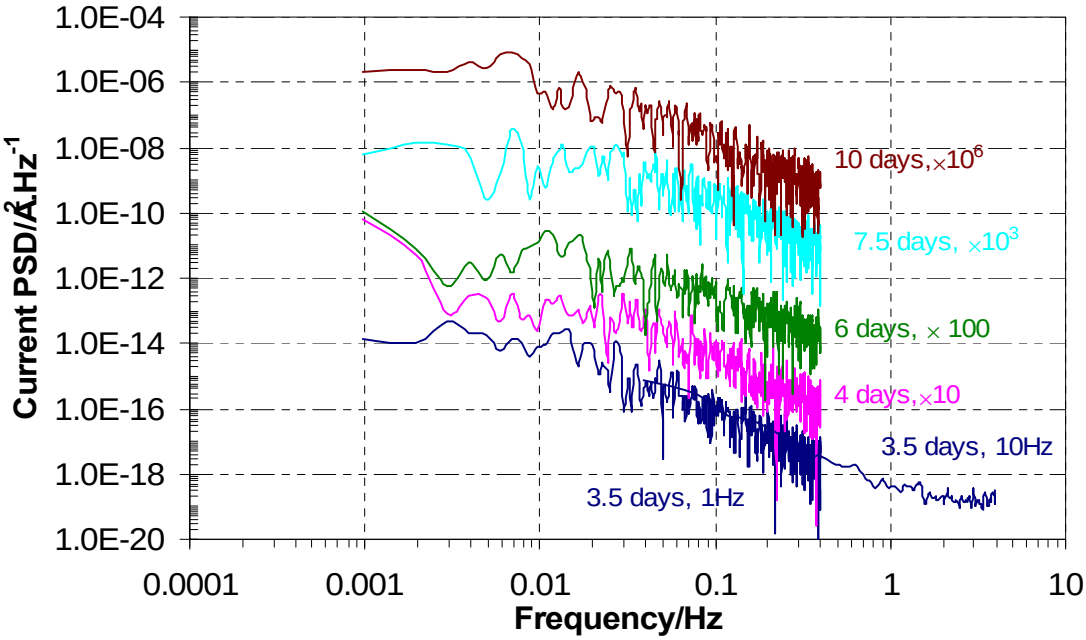

Figure 8. Current PSDs (FFT) with time for 1cm^2 coupons in 1% NaCl solution

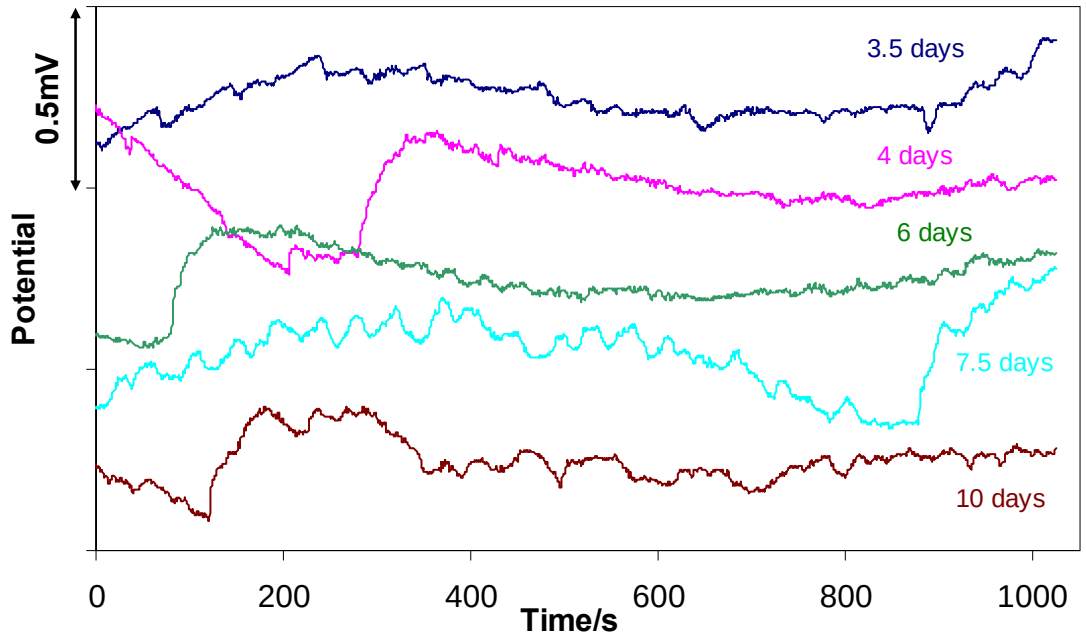

Figure 9. Potential noise with time for 11.6cm^2 coupons in 1% NaCl solution after removing the DC drift using the polynomial fitting method

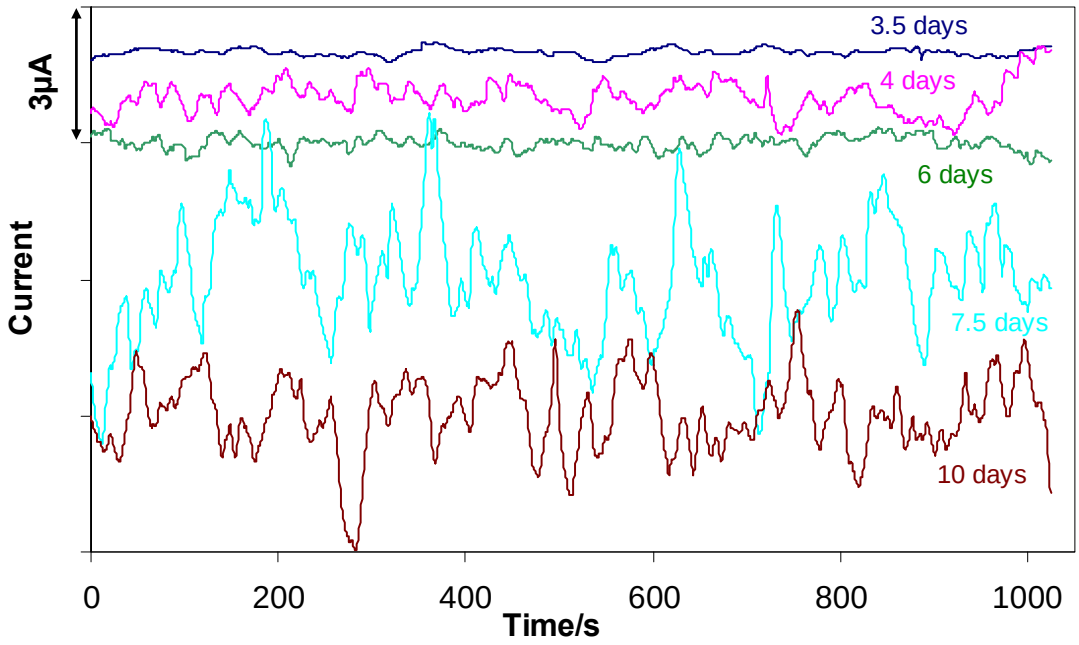

Figure 10. Current noise with time for 11.6cm^2 coupons in 1% NaCl solution after removing the DC drift using the polynomial fitting method

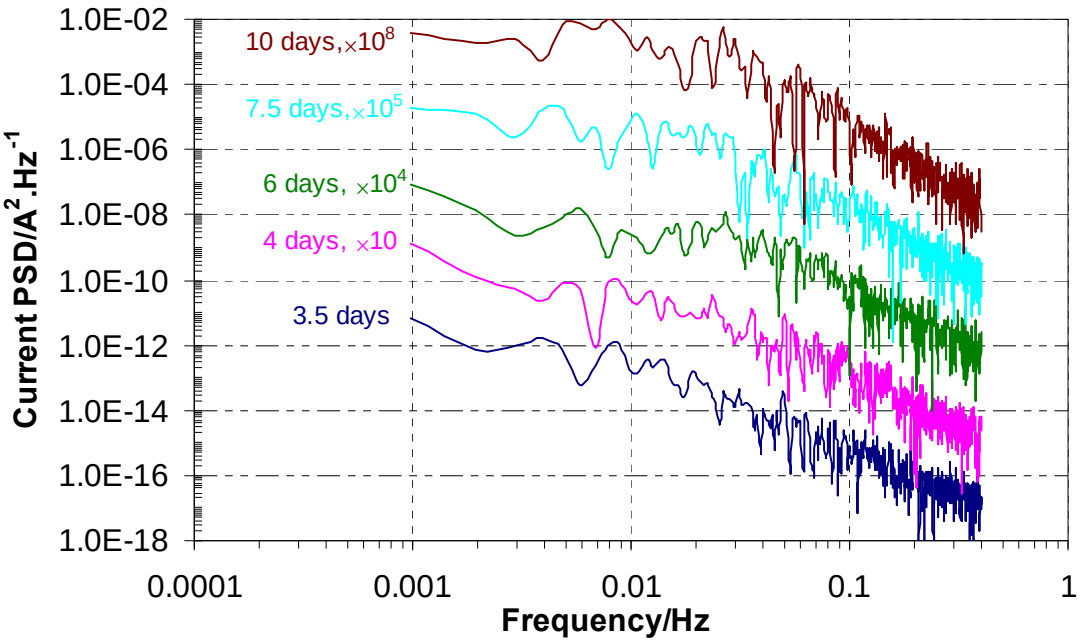

Figure 11. Current PSDs (FFT) with time for 11.6cm^2 coupons in 1% NaCl solution

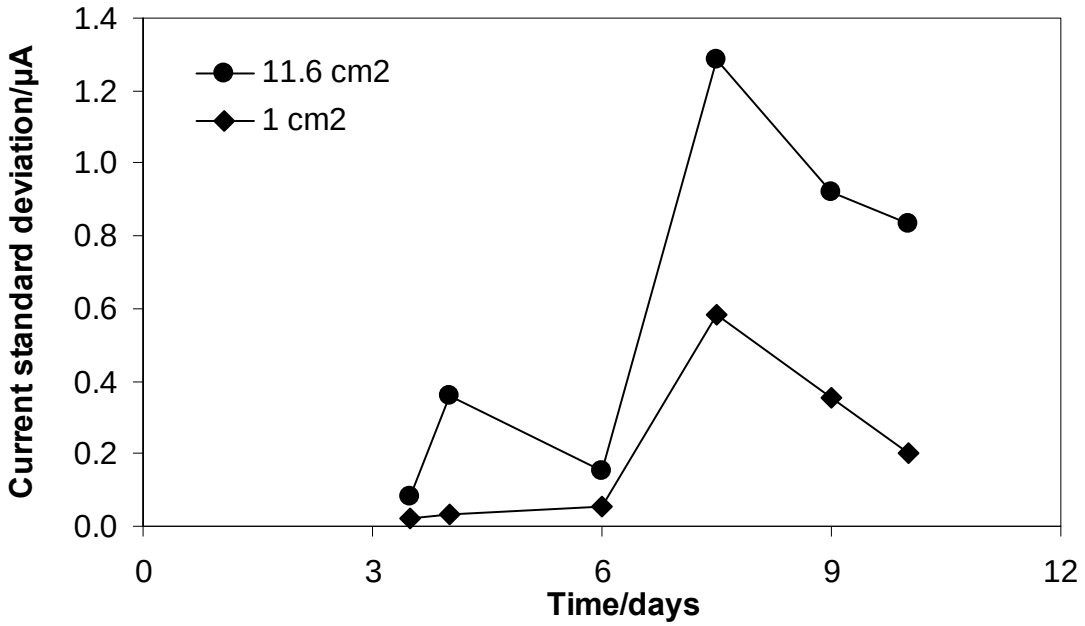

Figure 12. Current standard deviation with time for 11.6cm^2 and 1cm^2 coupons in 1% NaCl solution

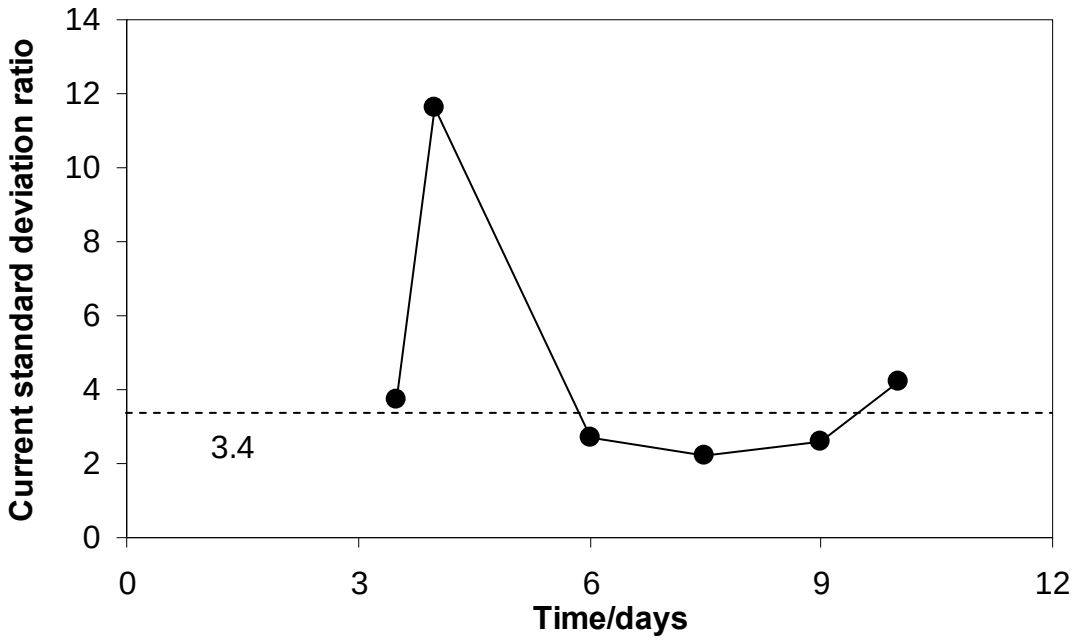

Figure 13. Current standard deviation ratio in 1% NaCl solution

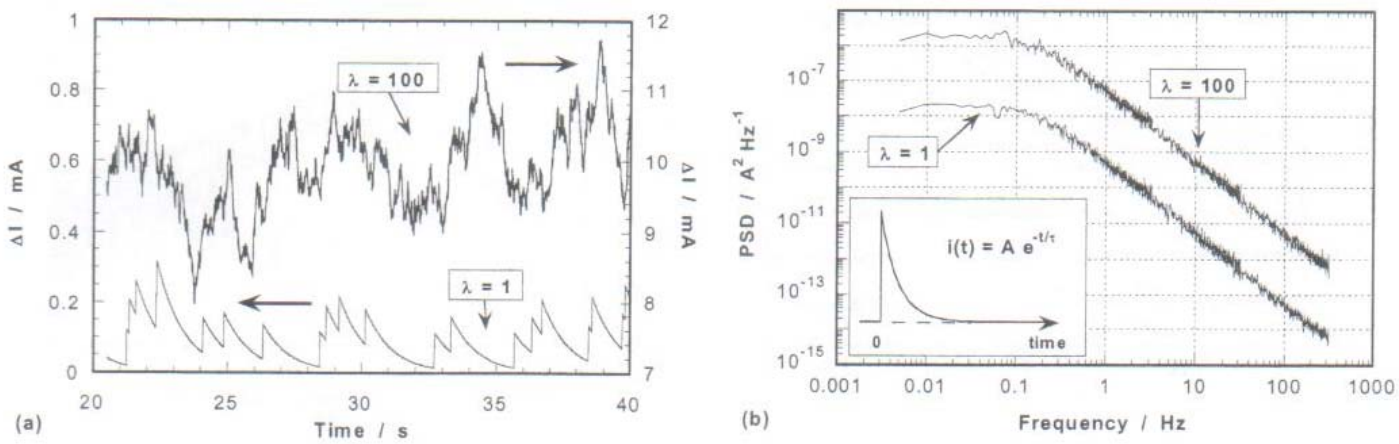

Figure 14. Influence of the number of transients on (a) the time record and (b) PSD. Simulations of randomly occurring exponentially decaying transients defined in the inset for two values of the transients average rate: $\lambda = 1$ and $100 s^{-1}$ ($A = 10^{-4}$ A, $\tau = 1$ s) [9]

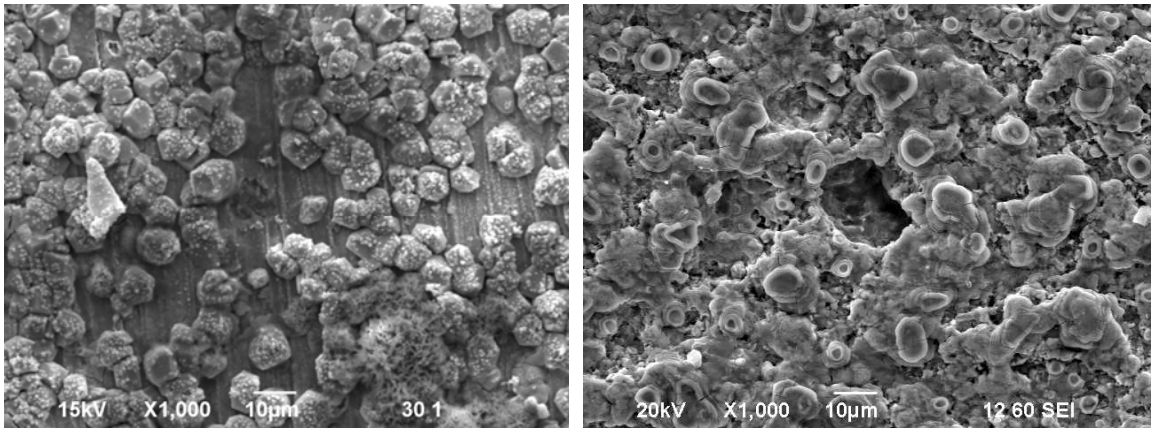

(a) (b)

Figure 15. Surface morphology for metal with film ((a)) and after film removal by using Clarke solution ((b)) after 8 days in 10% NaCl solution

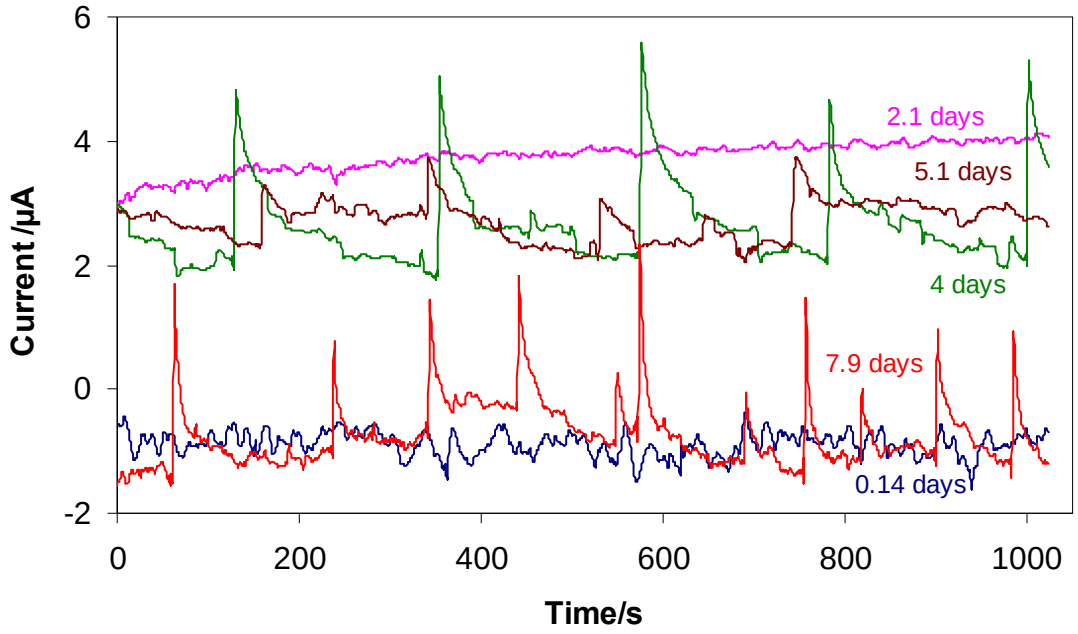

Figure 16. Current noise (raw data) with time in 10% NaCl solution

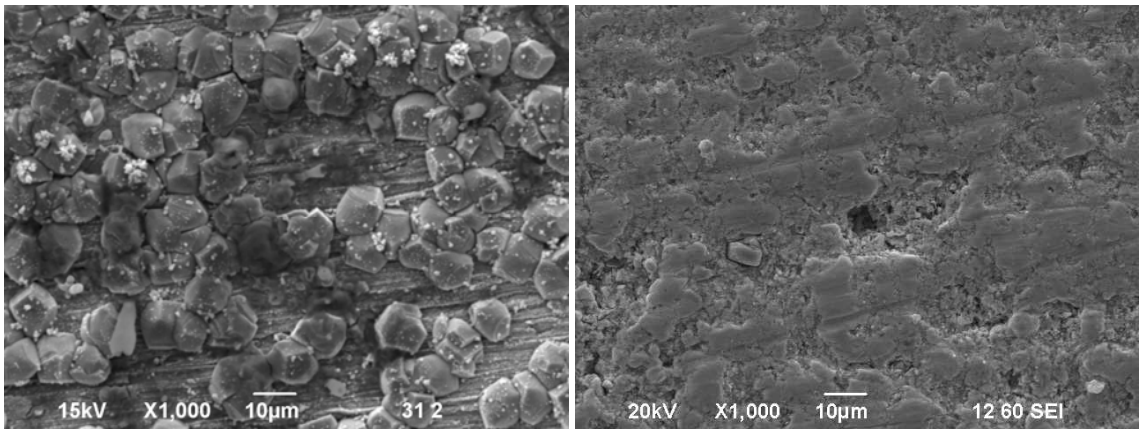

(a) (b)

Figure 17. Surface morphology for metal with film ((a)) and after film dissolve by using Clarke solution ((b)) after 8 days in 20% NaCl solution

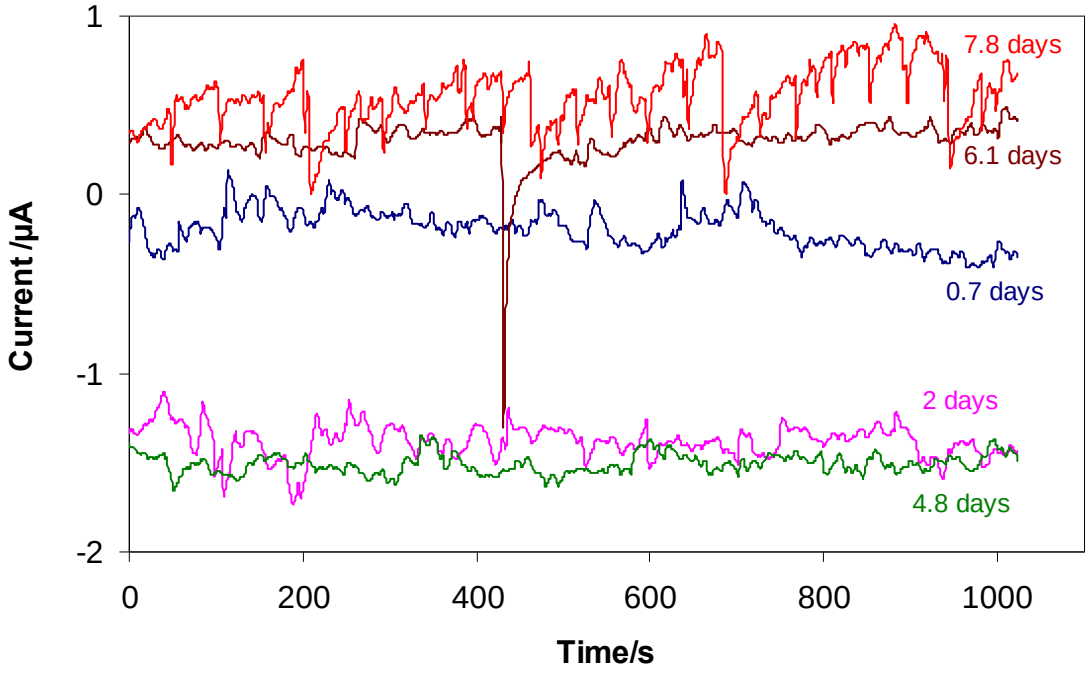

Figure 18. Current noise (raw data) with time in 20% NaCl solution

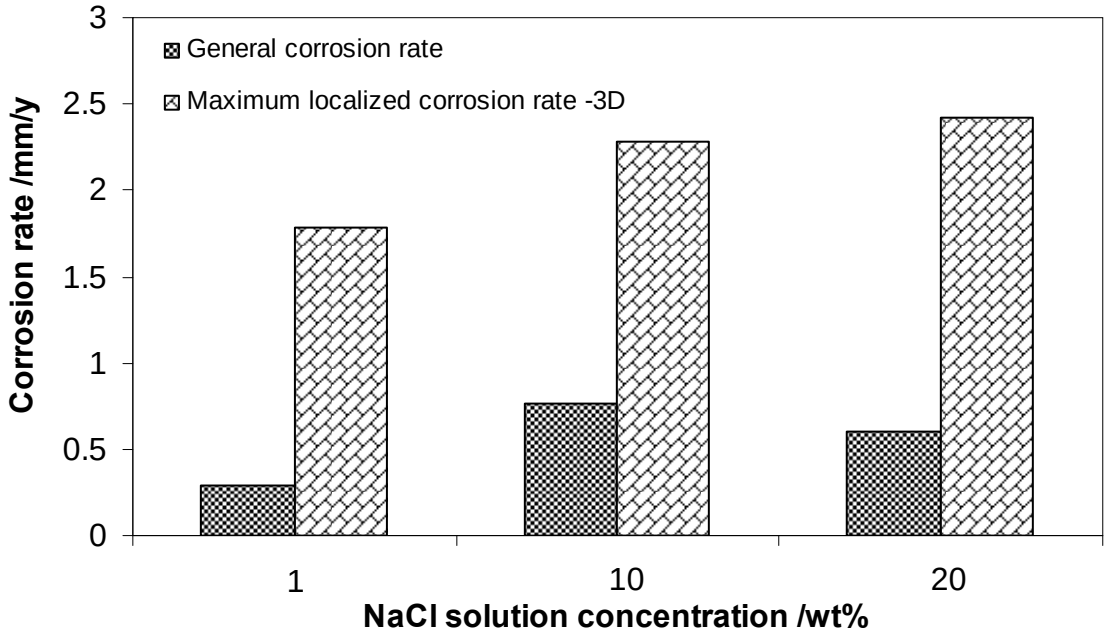

Figure 19. Variation of general corrosion rate and maximum localized corrosion rate with NaCl solution concentration after 8 days